Original Article

Regional homogeneity alterations in multifrequency bands in patients with extracranial multi-organ tuberculosis: a prospective cross-sectional study

Yichuan Wang[1,2#], Jianjie Wen[3,4#], Chengcheng Kong[1,2], Zexuan Xu[2], Su Hu[3,4], Mengting Li[3,4], Xinguang Wang[5], Hongqiang Zhang[6], Xize Jia[3,4,6], Qingguo Ding[6], Jili Wu[7], Dailun Hou[1,2]

[1]Department of Medical Imaging, Beijing Tuberculosis and Thoracic Tumor Research Institute, Beijing, China; [2]Department of Medical Imaging, Beijing Chest Hospital, Capital Medical University, Beijing, China; [3]School of Teacher Education, Zhejiang Normal University, Jinhua, China; [4]Key Laboratory of Intelligent Education Technology and Application of Zhejiang Province, Zhejiang Normal University, Jinhua, China; [5]School of Information Science and Electronic Technology, Jiamusi University, Jiamusi, China; [6]Department of Radiology, Changshu No. 2 People's Hospital, The Affiliated Changshu Hospital of Xuzhou Medical University, Changshu, China; [7]Department of Medical Imaging, Fourth People's Hospital of Taiyuan, Taiyuan, China

Contributions: (I) Conception and design: D Hou, Q Ding; (II) Administrative support: D Hou, X Jia; (III) Provision of study materials or patients: J Wu; (IV) Collection and assembly of data: Y Wang, C Kong, Z Xu; (V) Data analysis and interpretation: J Wen, S Hu, M Li, X Wang, H Zhang; (VI) Manuscript writing: All authors; (VII) Final approval of manuscript: All authors.

[#]These authors contributed equally to this work.

Correspondence to: Dailun Hou. Department of Medical Imaging, Beijing Tuberculosis and Thoracic Tumor Research Institute, Beijing, China; Department of Medical Imaging, Beijing Chest Hospital, Capital Medical University, 97 Ma Chang Street, Beijing 101149, China. Email: hou.dl@mail.ccmu.edu.cn; Jili Wu. Department of Medical Imaging, Fourth People's Hospital of Taiyuan, 231 Xikuang Street, Taiyuan 030053, China. Email: wujili9797@163.com; Qingguo Ding. Department of Radiology, Changshu No. 2 People's Hospital, The Affiliated Changshu Hospital of Xuzhou Medical University, 18 Taishan Street, Changshu 215500, China. Email: qingguo_d2015@163.com.

Background: This study aimed to clarify the spontaneous neural activity in the conventional frequency band (0.01–0.08 Hz) and 2 subfrequency bands (slow-4: 0.027–0.073 Hz; slow-5: 0.01–0.027 Hz) in patients with extracranial multi-organ tuberculosis (EMTB) through regional homogeneity (ReHo) analysis.

Methods: In all, 32 patients with EMTB and 31 healthy controls (HCs) were assessed by resting-state functional magnetic resonance imaging (rs-fMRI) scans to clarify the abnormal spontaneous neural activity through ReHo analysis in the conventional frequency band and 2 subfrequency bands.

Results: Compared with the HCs, the patients with EMTB exhibited decreased ReHo in the left postcentral gyrus [t=–4.79; 95% confidence interval (CI): –0.79 to –0.31] and the left superior cerebellum (t=–4.45; 95% CI: –0.54 to –0.21) in the conventional band. Conversely, increased ReHo was observed in the right middle occipital gyrus (t=3.94; 95% CI: 0.18–0.53). In the slow-4 band, patients with EMTB only exhibited decreased ReHo in the superior cerebellum (t=–4.69; 95% CI: –0.54 to –0.22); meanwhile, in the slow-5 band, these patients exhibited decreased ReHo in the right postcentral gyrus (t=–3.76; 95% CI: –0.74 to –0.21) and the left superior cerebellum (t=–5.20, 95% CI: –0.72 to –0.31). After Bonferroni correction, no significant correlation was observed between the ReHo values in clusters showing significant between-group differences and cognitive test scores.

Conclusions: ReHo showed abnormal synchronous neural activity in patients with EMTB in different frequency bands, which provides a novel understanding of the pathological mechanism of EMTB.

Keywords: Tuberculosis; extracranial multi-organ tuberculosis (EMTB); regional homogeneity (ReHo); resting-state functional magnetic resonance imaging (rs-fMRI); frequency-dependent

Submitted Mar 11, 2022. Accepted for publication Jan 04, 2023. Published online Feb 13, 2023.
doi: 10.21037/qims-22-229
View this article at: https://dx.doi.org/10.21037/qims-22-229

Introduction

Tuberculosis is an infectious disease caused by *Mycobacterium tuberculosis* (MTB), which can infect almost all organs in the human body. Tuberculosis is one of the leading causes of death from a single infectious agent (1). Intracranial tuberculosis is the most serious form of tuberculosis and is associated with high rates of mortality and morbidity, and a large proportion of patients with intracranial tuberculosis experience varying degrees of neurological sequelae (2-4). Meanwhile, delayed diagnosis and treatment are associated with a poor prognosis in intracranial tuberculosis (5). Despite significant improvements in computer tomography (CT) and magnetic resonance imaging (MRI) technology, it remains very challenging to diagnose intracranial tuberculosis at the early stage (6,7).

Intracranial tuberculosis could be unifocal or multifocal, and its common clinical symptoms include fever, headache, cognitive impairment, meningeal irritation, cranial nerve damage, and occupying effect, which are nonspecific and sometimes confusing (4,6). Many intracranial tuberculosis cases have been reported to cause considerable diagnostic difficulty due to confusing clinical signs and nontypical imaging features (8,9). Patients with multi-organ tuberculosis without intracranial lesions or with lesions that cannot be found in the current clinical examination are regarded as patients with extracranial multi-organ tuberculosis (EMTB), who may potentially develop intracranial tuberculosis (10). Accurate EMTB diagnosis could be helpful for the early intervention of intracranial tuberculosis (10). A positron emission tomography computed tomography (PET-CT) study of tuberculous encephalitis showed that ^{18}F-fluorodeoxyglucose (^{18}F-FDG) PET-CT could detect focal cortical hypermetabolism, while no visible lesion was observed on MRI in the same brain region, which could account for the neurological deficits beyond MRI perception. Additionally, follow-up scans showed improvement in the cortical hypermetabolism that corresponded with clinical improvement (11). Another recent study showed that patients with intracranial tuberculosis have functional alteration in the brain (12), Thus, patients with EMTB may have altered brain function with no detectable lesions, which may be a new direction to diagnose early intracranial tuberculosis. However, to date, the brain functional characteristics of these patients have not yet been explored, which limits the early diagnosis of intracranial tuberculosis to a certain extent. Therefore, it is necessary and urgent to use novel tools to explore the EMTB and identify reliable neuro-markers.

Resting-state functional magnetic resonance imaging (rs-fMRI), which relies on the blood-oxygen-level-dependent (BOLD) signal, is a promising avenue for clarifying the neural mechanism of various intrinsic brain disorders (13-16). The regional homogeneity (ReHo) method is a resting-state analytical method based on Kendall coefficient of concordance (KCC), which measures the similarity of several time series between a specific voxel and the nearest 26 voxels (17). ReHo analysis was developed and employed to extract the local synchronization feature of the spontaneous BOLD signal of the whole brain (17-19), which demonstrated that changes in ReHo values are related to abnormal brain activity (20). Increased ReHo indicates the increase in local brain consistency, and vice versa, demonstrating neuronal metabolic activity disorder (21). It has also been reported that ReHo can identify cerebral regions with abnormal brain function (22) and is widely used in clinical studies (23-25); it is especially suitable for brains with lesions (26). Moreover, ReHo has been demonstrated to have a high test-retest reliability in the study of the consistency of brain activity (18,27,28) and could serve as an efficient neuro-marker in identifying brain functional abnormalities in a variety of brain disorders (26,27,29), such as Alzheimer's disease (AD) (19,30), depression (31), bipolar disorder (BP) (32,33), and stroke (34,35). Previous studies have shown that some abnormal brain regions found using the ReHo method in patients with AD were consistent with some previous PET studies (36,37) and also reported AD-related increased activation during cognitive tasks (38), which may support the use of ReHo in revealing associations with brain diseases. ReHo has also been employed to detect the brain activities of patients with EMTB to identify abnormal brain regions and learn more about the pathology, pathophysiology, and mechanism of intracranial tuberculosis.

To date, most ReHo studies have focused on the conventional low-frequency band, which has a frequency of 0.01–0.08 Hz, as its BOLD signal is believed to reflect

spontaneous brain activity (39). However, studies have suggested that the results of a single frequency band cannot provide accurate frequency characteristics, while the neural oscillations of different frequencies may have distinct sensibilities to activity in various regions and can reflect the distinct physiological functions of brain activity (40,41). It has been demonstrated that the conventional low-frequency oscillation (0.01–0.08 Hz) can be further divided into the slow-4 frequency band (0.027–0.073 Hz) and the slow-5 frequency band (0.01–0.027 Hz), which are mainly related to gray matter. Slow-4 and slow-5 facilitate the identification of the correlations between functional processing and diseases (41,42). Frequency-dependent ReHo abnormalities in psychiatric and neurological diseases have been revealed in some studies. Zhao *et al.* reported that there was a significant ReHo variation in stroke-associated activities between the slow-4 and slow-5 frequency bands (35). In addition, Zhang *et al.* reported that tension-type headache patients showed highly resemblant altered ReHo regions in the conventional and slow-5 frequency bands, while no region showed significance in the slow-4 frequency band (43). In a study of cirrhotic patients, the slow-4 band exhibited higher correlations with blood ammonia level and neuropsychological performance, and patients with or without clinical hepatic encephalopathy could be more accurately differentiated (24). It seems that the altered ReHo values are modulated by the specific frequency bands.

Therefore, in this study, we applied ReHo at the conventional frequency band (0.01–0.08 Hz), slow-4 frequency band (0.027–0.073 Hz), and slow-5 frequency band (0.01–0.027 Hz) to examine the synchronization of local brain activity in patients with EMTB. We aimed to recognize the regional spontaneous brain activity in multifrequency bands of patients with EMTB compared with healthy controls (HCs) and to explore whether the abnormal intrinsic neural activity was associated with the specific frequency bands. In addition, these abnormal ReHo brain regions were also analyzed in relation to the patients' neurocognitive scores. We present the following article in accordance with the STROBE reporting checklist (available at https://qims.amegroups.com/article/view/10.21037/qims-22-229/rc).

Methods

Participants

This was a prospective, cross-sectional study. From September 2020 to July 2021, 32 patients with EMTB were recruited from the inpatient department and 31 HCs were recruited from the community through advertising. The HCs were matched in the aspects of sex, age, and education level. The inclusion criteria of both the patients with EMTB and HCs were as follows: (I) 18–60 years of age, (II) at least 6 years of education, (III) right-handed, (IV) no MRI contraindications, and (V) no history of psychiatric or neurological diseases.

Patients with EMTB were those who were infected in more than 1 organ by MTB, did not have intracranial tuberculosis, or had lesions that could not be found using the current clinical examinations. Pulmonary tuberculosis was diagnosed according to the Health Industry Standard of the People's Republic of China—Diagnosis for pulmonary tuberculosis (WS 288-2017) published in 2017 by the National Health and Family Planning Commission of China (44), and all of the patients met the criteria for confirmed cases. Patients were diagnosed with confirmed extrapulmonary tuberculosis if they met either of the following conditions: (I) positive acid-fast staining, MTB culture or GeneXpert MTB/RIF (Cepheid, Sunnyvale, CA, USA) urine assay, body fluid, secretion or tissue smear results (45); and (II) histopathological sections showing granulomatous inflammation, caseous necrosis in the center, Langhans cells in the periphery, and lymphocytes and fibrous connective tissue in the periphery (46). The exclusion criteria were as follows: (I) drug, nicotine, or alcohol abuse; (II) confirmed history of anxiety, hypertension, depression, diabetes, psychiatric disorders, or severe neurological disorders; (III) human immunodeficiency virus (HIV) infection, based on an HIV serum antibody exam; (IV) previous intracranial lesions detected by MRI or CT; (V) in the luteal phase of the menstrual cycle or pregnancy; (VI) claustrophobia; and (VII) head motion (maximal translation >3.0 mm and maximal rotation >3.0°).

One participant in the HC group was excluded from this study as the slice number was inconsistent with the other participants. Finally, 32 patients with EMTB and 30 HCs were enrolled (*Figure 1*). Meanwhile, the study period was set as 10 months because the sample size of participants met the demand for rs-fMRI according to previous studies (13,15,35,43). This study was conducted in accordance with the Declaration of Helsinki (as revised in 2013) and was approved by the Ethics Committee of Beijing Chest Hospital, Capital Medical University (No. YJS-2021-006). Informed consent was obtained from all individual participants.

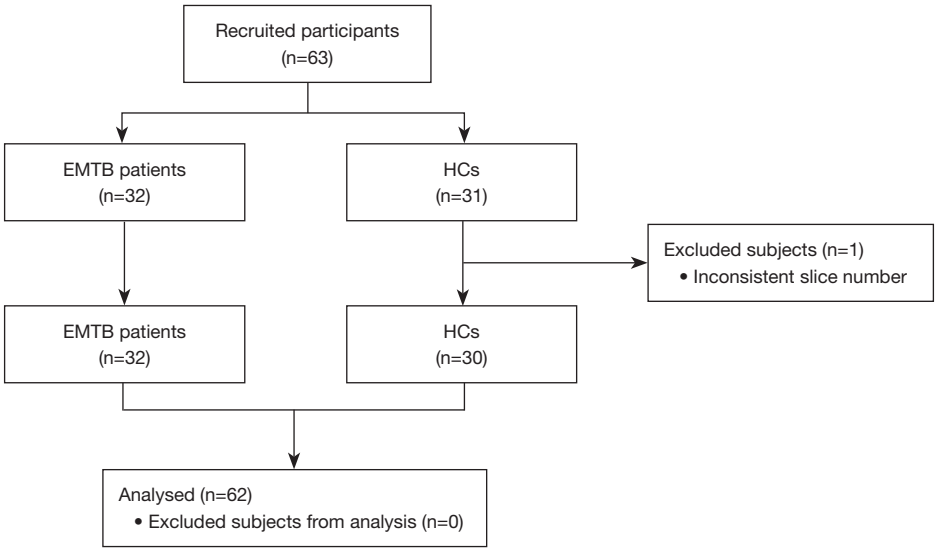

Figure 1 Enrolment flow diagram. EMTB, extracranial multi-organ tuberculosis; HCs, healthy controls.

Neurocognitive tests

All participants completed a set of standardized comprehensive neurocognitive tests. The neurocognitive tests were executed by the researchers, who were trained before this study to avoid inconsistency, and all the participants were tested in a quiet room at the department of radiology. The general cognitive levels were assessed using the Mini-Mental State Examination (MMSE) and the Montreal Cognitive Assessment (MoCA) (47,48). Executive function was measured using the Trail Making Test A and B (TMT-A and TMT-B); TMT-A was a test of visual search and motor speed skills, while test TMT-B demanded higher-level cognitive skills, such as mental flexibility (49). Visuospatial function was assessed using the Clock Drawing Test (CDT) (50). The Verbal Fluency Test (VFT) was employed to assess verbal ability and executive control and consisted of 2 parts: category fluency and letter fluency (51). The Digit Span Test (DST) was used to evaluate attention-concentration and working memory (52). Verbal memory was assessed using the Rey Auditory Verbal Learning Test (RAVLT) for immediate and delayed recall (52). Information processing speed was assessed using the Symbol Digit Modalities Test (SDMT) (52).

MRI scan acquisition

A 3T SIGNA Pioneer MRI scanner (GE Healthcare) with a 32-channel phased-array head–neck coil was employed, and scanning was performed after clinical data collection and neuropsychological tests in the MRI scanning room. During scanning, all of the participants were instructed to close their eyes and remain awake. The scanning parameters were as follows: (I) echo planar imaging for rs-fMRI, repetition time (TR) =3,000 ms, echo time (TE) =35 ms, slice =30, slice thickness =3.5 mm, interslice gap =0 mm, voxel size =3.8×3.8×3.5 mm^3, flip angle =90°, field of view (FOV) =240×240 mm^2, matrix size =64×64, and session period =6 min 24 s; (II) fast spoiled gradient-recalled imaging for high-resolution three-dimensional (3D) T1-weighted anatomical imaging, TR=7,400 ms, TE =1.0 ms, flip angle =9°, FOV =240×240 mm^2, matrix size =256×256, slice thickness =1.2 mm, interslice gap =0 mm, voxel size =0.9×0.9×1.2 mm^3, slice =252 slices, and session period =2 min 49 s. In addition, the T2-weighted images and T1-weighted fluid-attenuated inversion recovery (T1-FLAIR) images of 32 patients were collected to ensure that there were no lesions in the brains of patients with EMTB. The T2-weighted images and T1-FLAIR images are included in the supplementary materials (see Figures S1-S32 in for details).

Data preprocessing

Data preprocessing was performed using RESTplus, version 1.24 (http://www.restfmri.net) (Xize Jia, Hangzhou, China) (53), and Statistical Parametric Mapping (SPM12; https://www.fil.ion.ucl.ac.uk/spm) was conducted on the MATLAB

2017b platform (MathWorks). The main preprocessing procedures were as follows: (I) at the beginning of the scan, due to the possible presence of participants' maladaptation and uneven machine magnetic fields, the first 10 volumes of 128 volumes were removed to avoid interference by the circumstances; (II) owing to the time difference among the data at different time points, slice-timing correction was performed for inter-lice acquisition delay; (III) head-motion correction was conducted (cases with translation >3 mm or rotation >3° were defined as excessive motion; no participants were excluded due to excessive head motion); (IV) spatial normalization was applied on the Montreal Neurological Institute (MNI) space through the deformation fields derived from tissue segmentation (New Segment) of the structural images (resampling voxel size =3 mm × 3 mm × 3 mm); (V) the linear trend of the time course was removed; (VI) regression of nuisance covariates, including white matter (WM), cerebrospinal fluid (CSF), global signal, and head motion effects was achieved using the Friston 24-parameter model (54); and (VII) a temporal filter with a bandpass of the conventional frequency band (0.01–0.08 Hz), slow-4 band (0.027–0.073 Hz), and slow-5 band (0.01–0.027 Hz) was used.

ReHo calculations

ReHo was evaluated using RESTplus (version 1.24) based on the KCC. Specifically, the ReHo value was acquired by calculating the KCC of the time course of a given voxel and those of its nearest 26 voxels as follows (17):

$$W = \frac{\sum (R_i)^2 - n(\overline{R})^2}{\frac{1}{12}K^2(n^3 - n)} \quad [1]$$

where W denotes the KCC among specific voxels, ranging from 0 to 1; R_i denotes the sum rank of the ith time point; $\overline{R} = ((n+1)K)/2$ denotes the mean of the R_i's; K denotes the number of time series within a measured cluster (K=7, K=19, and K=27, respectively; 27 in the current study); and n denotes the number of ranks.

Next, the voxel-wise ReHo was standardized by the ReHo value for each voxel and was subtracted from the mean ReHo value for the whole brain, with the result being divided by the standard deviation (SD). Normalization has been shown to improve the normality and reliability of amplitude (41). To reduce the spatial noise, spatial smoothing [full-width at half-maximum (FWHM) =6 mm] was conducted on the ReHo z-maps after ReHo calculation.

Statistical analysis

Neuropsychological test scores and demographic data were acquired and compared using SPSS 25.0 (IBM Corp.). Group differences, including age, education years, and neuropsychological test scores between the patients with EMTB and HCs were investigated using independent samples t-tests, while the χ^2 test was employed for the estimation of intergroup sex differences. P<0.05 was considered statistically significant.

To compare the ReHo of the EMTB and HC groups, the whole brain was examined using a 2-sample t-test in the 3 different frequency bands mentioned above using RESTplus (version 1.24). The T-maps obtained were corrected using the Gaussian random field (GRF) theory (55), and brain regions were reported at the significant level of a threshold of the two-tailed voxel-level P<0.005 and cluster-level P<0.05 with GRF correction.

Finally, we further correlated the mean ReHo values in each brain region that showed significant between-group differences through the neuropsychological tests, including the MMSE, MoCA, TMT-A, TMT-B, CDT, VFT, DST forward, DST backward, RAVLT-I, RAVLT-II, RAVLT, and SDMT by using Pearson correlation coefficient, aiming to investigate the relationship between the regional spontaneous brain activity and the clinical symptoms of EMTB. The correlation analysis was conducted using SPSS 25.0, and P<0.05 was considered statistically significant. In addition, we also applied Bonferroni correction in the correlation analyses.

Results

Demographic and clinical features of the participants

The distribution of EMTB sites is shown in *Table 1*. Among the patients with EMTB, the most common sites of tuberculosis disease included pulmonary (100.0%), polyserositis (46.9%), osteoarticular (31.3%), and lymphatic (31.3%) sites. The most common EMTB was pulmonary tuberculosis complicated with tuberculous polyserositis (15 cases, 46.9%), followed by pulmonary tuberculosis complicated with osteoarticular tuberculosis (10 cases, 31.3%).

There were no statistical differences between the 2 groups in terms of age (P=0.508), gender (P=0.570), or educational level (P=0.702). The EMTB group exhibited diminished performance in MMSE (P=0.046) and VFT (P=0.019), while no significant intergroup differences were observed in the other neuropsychological tests. The details are presented in *Table 2*. We also compared the subscores of

Table 1 Sites of EMTB

System	Organ	Number of patients (%)
Pulmonary		32 (100.0)
	Lung	32 (100.0)
Polyserositis		15 (46.9)
	Pleura	11 (34.4)
	Peritoneum	6 (18.8)
	Pericardium	2 (6.3)
Osteoarticular		10 (31.3)
	Thoracic spine	5 (15.6)
	Lumbar spine	3 (9.4)
	Hip joint	1 (3.1)
	Sacroiliac joint	1 (3.1)
	Knee joint	1 (3.1)
Lymphatic		10 (31.3)
	Cervical	8 (25.0)
	Axillary	2 (6.3)
Intestinal		4 (12.5)
	Colon	4 (12.5)
Soft tissue		3 (9.4)
	Skin	3 (9.4)
Testicular		1 (3.1)
	Testis	1 (3.1)
Urinary system		1 (3.1)
	Bladder	1 (3.1)

The first line of every system is the total number of patients infected in this system, and the following lines represents the number of patients infected in each organ of this system. More than 1 organ was infected in a system in some patients with EMTB, and thus, the total number of organs could be larger than the number for a system. EMTB, extracranial multi-organ tuberculosis.

MMSE and MoCA, and the patients with EMTB performed worse in the Place Orientation of MMSE (P=0.001), while other scores showed no significant differences. The complete results are shown in the supplementary materials (see Table S1 for details). In addition, the demographics and cognitive tests scores are also available in the supplementary materials (available at https://cdn.amegroups.cn/static/public/qims-22-229-1.xlsx).

Group differences in ReHo in different frequency bands

Compared with the HCs, patients with EMTB showed decreased ReHo values in the left postcentral gyrus [Postcentral_L; t=–4.79; 95% confidence interval (CI): –0.79 to –0.31; 2-tailed, voxel-level P<0.005; cluster-level P<0.05, GRF correction] and the left superior cerebellum (Cerebellum_Crus1_L; t=–4.45; 95% CI: –0.54 to –0.21; 2-tailed, voxel-level P<0.005; cluster-level P<0.05; GRF correction) in the conventional band (0.01–0.08 Hz). Conversely, higher ReHo values were observed in the right middle occipital gyrus (Occipital_Mid_R; t=3.94, 95% CI: 0.18–0.53; 2-tailed, voxel-level P<0.005; cluster-level P<0.05, GRF correction) (*Table 3*, *Figure 2A*).

In the slow-4 band (0.027–0.073 Hz), only 1 cluster exhibited a significant decrease relative to the HC group in the superior cerebellum (Cerebellum_Crus1_L; t=–4.69; 95% CI: –0.54 to –0.22, 2-tailed, voxel-level P<0.005; cluster-level P<0.05, GRF correction) (*Table 3*, *Figure 2B*).

In the slow-5 band (0.01–0.027 Hz), 2 clusters exhibited significant decreases relative to the HC group in the right postcentral gyrus (Postcentral_R; t=–3.76, 95% CI: –0.74 to –0.21; 2-tailed, voxel-level P<0.005; cluster-level P<0.05, GRF correction) and the left superior cerebellum (Cerebellum_6_L; t=–5.20; 95% CI: –0.72 to –0.31, 2-tailed, voxel-level P<0.005; cluster-level P<0.05, GRF correction) (*Table 3*, *Figure 2C*).

All brain regions mentioned above were identified by the Anatomical Automatic Labeling (AAL) (57) template offered by the MNI using RESTplus (version 1.24).

To demonstrate the stability of the results, we performed ReHo analysis using RESTplus (version 1.25), and the results are shown in the supplementary materials (see Figure S33 in the supplementary materials for details). In addition, the uncorrected *T*-maps, ReHo maps, and pictures for the normalization of every participant are available online (see http://restfmri.net/Data_for_EMTB.zip for details).

Correlation analysis

In the conventional band (0.01–0.08 Hz), the ReHo value of the left postcentral gyrus in patients with EMTB was correlated with the DST forward score (r=0.536; uncorrected P=0.002), the DST backward score (r=0.404; uncorrected P=0.022), the RAVLT-I score (r=0.393; uncorrected P=0.026), the RAVLT-II score (r=0.402; uncorrected P=0.023), the RAVLT score (r=0.406; uncorrected P=0.021), and the SDMT score (r=0.425;

Table 2 Demographics and clinical characteristics of the study participants

Demographics	EMTB	HC	P value
Age (year)	33.69±10.33	35.77±13.86	0.508
Gender (male/female)	18/14	19/11	0.570[a]
Education (year)	11.50±3.60	11.17±3.21	0.702
MMSE	27.72±3.59	29.13±1.28	0.046
MoCA	24.69±4.32	25.90±2.82	0.199
TMT-A (s)	45.63±28.98	37.77±17.49	0.205
TMT-B (s)	113.35±61.43	103.53±66.50	0.552
CDT	4.63±0.66	4.73±0.45	0.456
VFT	38.34±13.25	45.7±10.50	0.019
DST forward	11.59±3.06	10.87±1.98	0.274
DST backward	7.78±2.95	8.33±2.77	0.451
RAVLT-I	43.22±10.64	46.37±11.38	0.265
RAVLT-II	10.00±3.55	9.93±3.59	0.942
RAVLT	53.22±13.82	56.30±14.43	0.394
SDMT	50.28±13.15	50.10±13.53	0.958

[a], χ^2 test for sex (n). The values are presented as mean ± SD. EMTB, extracranial multi-organ tuberculosis; HC, healthy control; MMSE, Mini-Mental State Examination; MoCA, Montreal Cognitive Assessment; TMT, Trail Making Test; s, second; CDT, Clock Drawing Test; VFT, Verbal Fluency Test; DST, Digital Span Test; RAVLT-I, Rey Auditory Verbal Learning Test (immediate recall); RAVLT-II, Rey Auditory Verbal Learning Test (delayed recall); RAVLT, Rey Auditory Verbal Learning Test (total score); SDMT, Symbol-Digit Modalities Test.

Table 3 Differences in the ReHo values in brain regions between the 2 groups

Number	Regions (AAL)	Region (Brodmann)	Cluster size	Peak t value	MNI coordinate (mm)			Effect size
					X	Y	Z	
Conventional band (0.01–0.08 Hz)								
Cluster 1	Cerebellum_Crus1_L	18	535	−4.45	−12	−75	−24	1.1489
Cluster 2	Occipital_Mid_R	19	153	3.94	36	−87	27	1.0175
Cluster 3	Postcentral_L	40	160	−4.79	−42	−30	45	1.2370
Slow-4 band (0.027–0.073 Hz)								
Cluster 4	Cerebellum_Crus1_L	18	143	−4.69	−15	−75	−27	1.2114
Slow-5 band (0.01–0.027 Hz)								
Cluster 5	Cerebellum_6_L	18	539	−5.20	−18	−57	−21	1.3442
Cluster 6	Postcentral_R	6	154	−3.76	57	−12	33	0.9704

Cluster size: the number of the voxels of the cluster showing significant differences; MNI coordinate: the coordinate of the voxel with the highest T value in the cluster; effect size: an indicator to measure the strength of experimental effects or variable correlation (56). ReHo, regional homogeneity; AAL, Anatomical Automatic Labeling; MNI, Montreal Neurological Institute; Cerebellum_Crus1_L, left superior cerebellum; Occipital_Mid_R, right middle occipital gyrus; Postcentral_L, left postcentral gyrus; Cerebellum_6_L, left superior cerebellum; Postcentral_R, right postcentral gyrus.

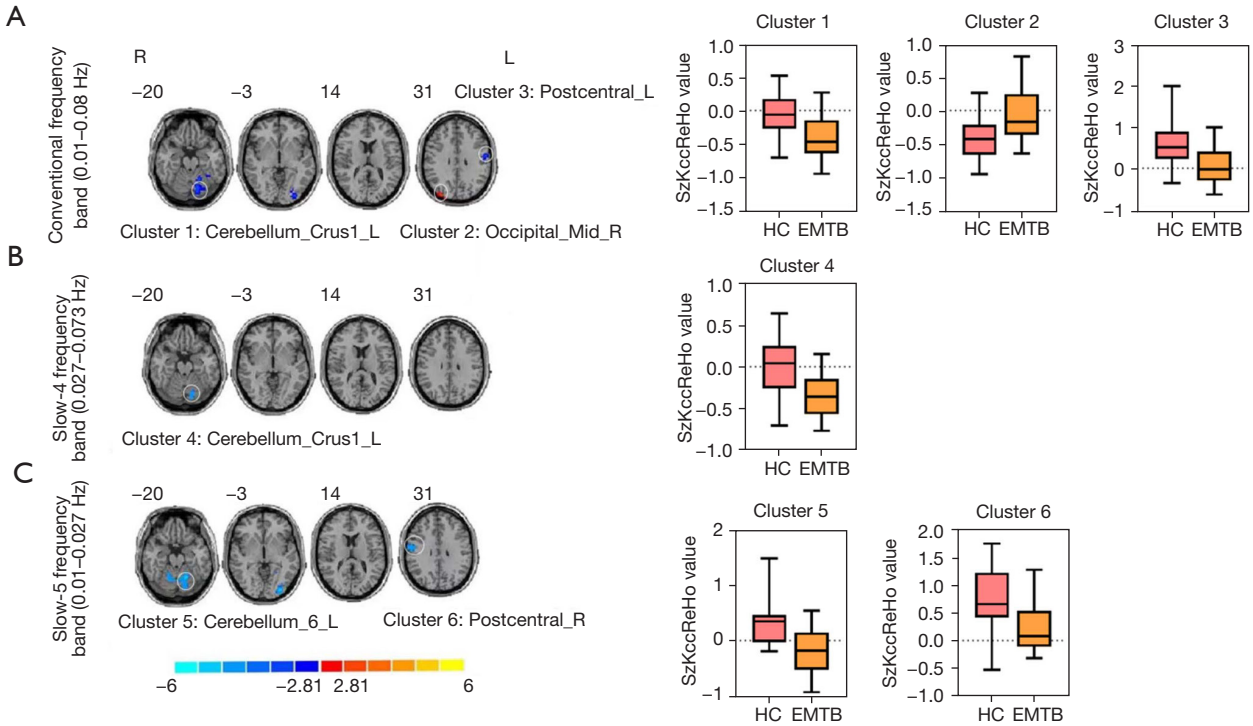

Figure 2 Brain regions with altered ReHo in different frequency bands in patients with EMTB and bar graphs of mean ReHo values of significant clusters in patients with EMTB and HCs in different frequency bands (2-tailed, voxel-level P<0.005; cluster-level P<0.05, GRF correction). RESTplus (version 1.24) software was used for calculation, and the AAL structural template was used for the render. More details of these regions are described in *Table 2*. (A) Brain regions showing differences in ReHo values between patients with EMTB and HCs and bar graphs of mean ReHo value of significant clusters in patients with EMTB and HCs in the conventional band (0.01–0.08 Hz). (B) Brain regions showing differences in ReHo values between patients with EMTB and HCs and bar graphs of mean ReHo values of significant clusters in patients with EMTB and HCs in the slow-4 band (0.027–0.073 Hz). (C) Brain regions showing differences in ReHo values between patients with EMTB and HCs and bar graphs of mean ReHo values of significant clusters in patients with EMTB and HCs in the slow-5 band (0.01–0.027 Hz). Cerebellum_Crus1_L, left superior cerebellum; Occipital_Mid_R, right middle occipital gyrus; Postcentral_L, left postcentral gyrus; Cerebellum_6_L, left superior cerebellum; Postcentral_R, right postcentral gyrus; ReHo, regional homogeneity; EMTB, extracranial multi-organ tuberculosis; GRF, Gaussian random field; AAL, Anatomical Automatic Labeling; HC, healthy control; ;SzKCCReHo, S refers to smoothing, z refers to standardization, KCC refers to Kendall coefficient of concordance.

uncorrected P=0.015) (*Figure 3*).

In the slow-5 band (0.01–0.027 Hz), the ReHo value of the right postcentral gyrus showed significant positive correlations with the DST forward score (r=0.447; uncorrected P=0.01) and the DST backward score (r=0.370; uncorrected P=0.037) (*Figure 4*).

Only the results of significant correlations are presented above, and the complete results of the correlation analysis and the scatter plots of results that were not significantly correlated are provided in the supplementary materials (see Table S2 and Figures S34-S39 in the supplementary materials for details).

However, the correlation analysis with Bonferroni correction showed no significant correlation between the altered ReHo values of patients with EMTB and all neuropsychological test scores.

Discussion

The present study is first of its kind to employ ReHo to clarify the spontaneous neural activities of patients with EMTB at resting states in the conventional frequency band (0.01–0.08 Hz) and 2 subfrequency bands (slow-4: 0.027–0.073 Hz; slow-5: 0.01–0.027 Hz). In the conventional frequency band, patients with EMTB exhibited decreased ReHo in the left postcentral gyrus and

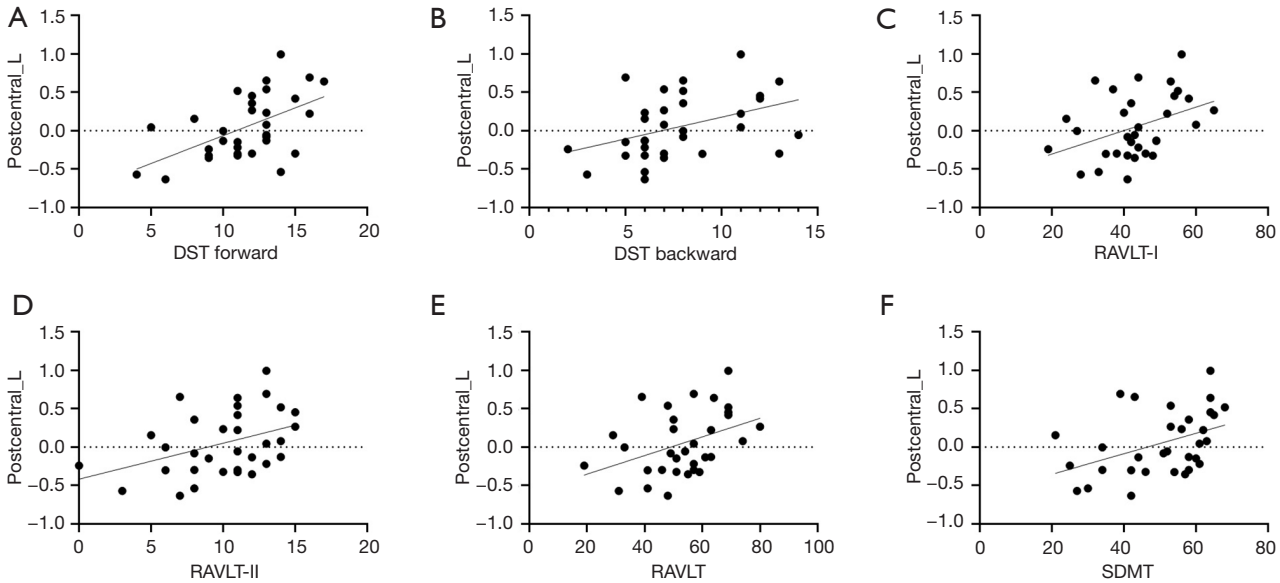

Figure 3 The correlation between the ReHo value of the left postcentral gyrus in patients with EMTB in the conventional band and neuropsychological test scores. (A) Correlation between ReHo values and DST forward scores. (B) Correlation between ReHo values and DST backward scores. (C) Correlation between ReHo values and RAVLT-I scores. (D) Correlation between ReHo values and RAVLT-II scores. (E) Correlation between ReHo values and RAVLT scores. (F) Correlation between ReHo values and SDMT scores. Postcentral_L, left postcentral gyrus; DST, Digital Span Test; RAVLT-I, Rey Auditory Verbal Learning Test (immediate recall); RAVLT-II, Rey Auditory Verbal Learning Test (delayed recall); RAVLT, Rey Auditory Verbal Learning Test (total score); SDMT, Symbol-Digit Modalities Test; ReHo, regional homogeneity; EMTB, extracranial multi-organ tuberculosis.

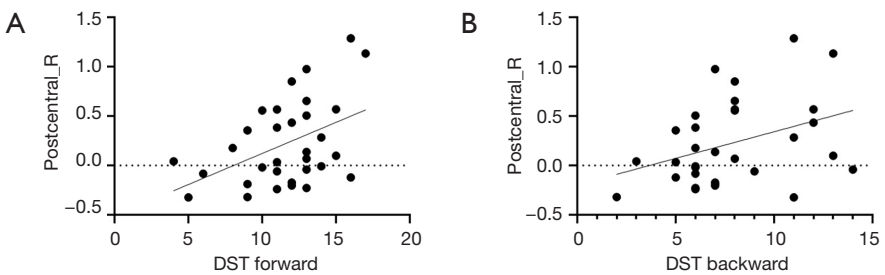

Figure 4 The correlation between the ReHo value of right postcentral gyrus in patients with EMTB in the slow-5 band and neuropsychological test scores. (A) Correlation between the ReHo values and DST forward scores, (B) Correlation between the ReHo values and DST backward scores. Postcentral_R, right postcentral gyrus; DST, Digital Span Test; ReHo, regional homogeneity; EMTB, extracranial multi-organ tuberculosis.

the left superior cerebellum and increased ReHo in the right middle occipital gyrus. A decreased ReHo value in the left superior cerebellum was also observed in the slow-4 band, but the cluster contained fewer voxels. In the slow-5 band, 2 additional regions exhibited decreased ReHo values in the right postcentral gyrus and the left superior cerebellum. Additionally, correlation analysis without multiple comparisons corrections showed a significant correlation between the ReHo value of the left postcentral gyrus in the conventional band and the right postcentral gyrus in the slow-5 band and some neuropsychological test scores. However, the correlation analysis results after the Bonferroni correction showed no significant correlation. This study demonstrates the advantages of subfrequency

band analyses and the frequency-dependent characteristics of ReHo alteration for patients with EMTB.

In the present study, compared with HCs, patients with EMTB had reduced ReHo values in the left postcentral gyrus in the conventional band, suggesting lower synchronization in the brain region. The postcentral gyrus is the somatosensory cortex, which is highly connected to other areas of the brain (58) and has numerous functions, including representation of the body, tactile attention, sensorimotor integration, and others (59). The reduced ReHo of the postcentral gyrus may be involved in pain processing, as patients with EMTB could experience persistent pain of the lesions in a clinical setting (1,60), which is supported by several studies on acute eye pain (61), low back pain (62), and trigeminal neuralgia (63). Furthermore, studies on the amplitude of low-frequency fluctuation (ALFF) also support the relevance of persistent pain to the postcentral gyrus (64,65). Meanwhile, we observed that the ReHo value of the left postcentral gyrus in patients with EMTB was correlated with the DST, RAVLT, and SDMT scores, which measure attention-concentration and working memory, verbal memory, and information processing speed, respectively. We thus deduced that the reduced synchronization of the postcentral gyrus in patients with EMTB might also relate to neurocognitive performance. This observation was consistent with previous studies reporting that the postcentral gyrus was associated with cognitive abilities (66,67). In addition, patients with EMTB performed worse in MMSE and VFT, indicating a lower general cognitive level as well as poorer verbal ability and executive control, illustrating the impairment of cognitive ability in patients with EMTB. In progressing to tuberculosis meningitis, patients could show cognitive impairment, motor deficits, and optic atrophy (2,68). A study on mice also reported that those with progressive pulmonary tuberculosis were observed to have cognitive impairment even in the absence of brain infection (69). Therefore, the decreased ReHo in the left postcentral gyrus of patients with EMTB may relate to pain and cognitive function; however, the mechanism of the relationship between the postcentral gyrus and cognitive abilities in patients with EMTB is still unclear and requires further study in the future.

An increased ReHo value was detected in the right middle occipital gyrus, suggesting abnormal synchronization. The middle occipital gyrus is located in the visual processing center, whose function is to synthesize visual information (70). Previous studies reported that the increased ReHo value of the middle occipital gyrus may be related to decreased vision (71) and contralateral visual compensation (72). Ocular tuberculosis could lead to a significant decrease in visual functions (73), and patients with intracranial tuberculosis may experience symptoms including diplopia and visual disturbance (74). In some cases, early-stage EMTB may also be accompanied by intracranial or ocular lesions that cannot be detected clinically (7,75), which influences visual ability. However, compared with HCs, patients with EMTB in this study did not show significantly worse visual ability, which may be because the enhanced consistency of the right middle occipital gyrus was present to compensate for impairment in visual processing in the other parts so that patients with EMTB could perform with almost normal vision. Thus, it was speculated that the increased ReHo value in the right middle occipital gyrus in patients with EMTB might be related to the potential visual impairment and the compensatory mechanism.

It has been demonstrated that the cerebellum is involved in cognition and that its lesions may cause cognitive dysfunction (76). A single-photon emission CT (SPECT) study reported that attention and visual space function are the key cognitive functions of the left cerebellum (77). Moreover, patients with EMTB had lower CDT scores and higher TMT scores, which might denote poorer executive function and visuospatial function. Furthermore, MTB is able to infect the cerebellum, as illustrated in a case report from Brazil involving a 52-year-old man with intracranial tuberculosis who had multiple lesions in the left cerebellum (78). This might play an important role in changing the function of the cerebellum in patients with EMTB. However, cerebellum lesions are always accompanied by lesions in the cerebrum and meninges, and it is difficult to identify the alterations caused by cerebellum lesions. This study suggested the potential role of the cerebellum in patients with EMTB, but the association between altered ReHo value and cognitive impairment in patients with EMTB requires further investigation.

Notably, the alterations in spontaneous brain activity in patients with EMTB were correlated with the specific frequency bands. Specifically, ReHo decreases were identified in the right postcentral gyrus in the slow-5 band but not in the slow-4 band. Furthermore, patients with EMTB had a greater decreased cluster in the left superior cerebellum in the ReHo in the slow-5 band compared with the slow-4 band, which may be attributed to the primary presence of gray matter–related oscillations in the slow-4 and slow-5 bands. It has also been indicated that the slow-4 and slow-5 bands have dissimilar levels of sensitivity to

different brain disorders (41). For instance, the slow-4 band provides greater diagnostic information for the pediatric hyperactivity disorder of attention deficit than do the other bands (79), while the slow-5 band is more sensitive to the abnormalities of spontaneous brain activities in mild cognitive impairment (80). In this study, compared with the slow-4 band, the slow-5 band was more sensitive to ReHo alterations in patients with EMTB and may provide novel information.

We further found that patients with EMTB exhibited abnormal brain function in some brain regions and performed worse in some cognitive tests. In clinical practice, CT and conventional MRI are the most commonly used tools to screen brain lesions in patients with EMTB, but their sensitivities in the early stage are insufficient (6,74,81). Patients with EMTB have functional deficits with no detectable lesions (11), which, according to our results, may relate to the clinical symptoms. We hope that the present study provides more information for diagnosis and treatment. Patients with EMTB need more care, and greater attention should be paid to their brain functional changes.

This study had some limitations that should be noted. First, no significant correlation between the ReHo value and neurocognitive test performance of the patients with EMTB was observed with Bonferroni correction, which may be attributable to the small sample size. Thus, a larger sample size is required in future studies to validate our results. Second, the dynamic changes in ReHo during different progressions in patients with EMTB could not be detected owing to the presence of cross-sectional group data. Third, the present study only employed voxel-wise ReHo analysis; given that the surface-based ReHo has advantages that allow it to reflect the functional organization of the cortex more specifically and it is influenced less by the noise of physiological activities (18,20,82,83), we should apply this method in our future studies. Fourth, although ReHo is widely used to explore brain diseases in the clinic, there is a lack of direct evidence of a relationship between ReHo and diseases, and we hope that this relationship can be revealed in future studies.

Conclusions

In this study, ReHo analysis was employed to investigate and compare the resting-state brain functions between the EMTB and HC groups in the conventional frequency band (0.01–0.08 Hz) and 2 subfrequency bands (slow-4: 0.027–0.073 Hz; slow-5: 0.01–0.027 Hz). The results revealed altered spontaneous brain activity in patients with EMTB, which was frequency-dependent. In addition, the altered ReHo values in patients with EMTB may be related to different clinical symptoms and neurocognitive impairments. This preliminary study facilitates exploration of the pathophysiological mechanism of EMTB in terms of objective imaging. Additionally, the ReHo abnormalities in patients with EMTB were clarified for the first time, which advances our understanding of the pathophysiology of EMTB.

Acknowledgments

We would like to thank all patients, volunteers, and research assistants who participated in this study.
Funding: This study was supported by the Leading Talents of Beijing Tongzhou District High Level Talent Development Support Project (No. YHLD2019029), the Talent Introduction Project of Beijing Chest Hospital, Capital Medical University (No. 2019-3), and the National Natural Science Foundation of China (No. 82001898).

Footnote

Reporting Checklist: The authors have completed the STROBE reporting checklist. Available at https://qims.amegroups.com/article/view/10.21037/qims-22-229/rc

Conflicts of Interest: All authors have completed the ICMJE uniform disclosure form (available at https://qims.amegroups.com/article/view/10.21037/qims-22-229/coif). The authors have no conflicts of interest to declare.

Ethical Statement: The authors are accountable for all aspects of the work in ensuring that questions related to the accuracy or integrity of any part of the work are appropriately investigated and resolved. This study was conducted in accordance with the Declaration of Helsinki (as revised in 2013) and was approved by the Ethics Committee of Beijing Chest Hospital, Capital Medical University (No. YJS-2021-006). Informed consent was obtained from all individual participants.

References

1. Sharma SK, Mohan A, Kohli M. Extrapulmonary tuberculosis. Expert Rev Respir Med 2021;15:931-48.
2. Kalita J, Misra UK, Ranjan P. Predictors of long-term neurological sequelae of tuberculous meningitis: a multivariate analysis. Eur J Neurol 2007;14:33-7.
3. Thakur K, Das M, Dooley KE, Gupta A. The Global Neurological Burden of Tuberculosis. Semin Neurol 2018;38:226-37.
4. Wen L, Li M, Xu T, Yu X, Wang L, Li K. Clinical features, outcomes and prognostic factors of tuberculous meningitis in adults worldwide: systematic review and meta-analysis. J Neurol 2019;266:3009-21.
5. Wilkinson RJ, Rohlwink U, Misra UK, van Crevel R, Mai NTH, Dooley KE, Caws M, Figaji A, Savic R, Solomons R, Thwaites GE; . Tuberculous meningitis. Nat Rev Neurol 2017;13:581-98.
6. Schaller MA, Wicke F, Foerch C, Weidauer S. Central Nervous System Tuberculosis : Etiology, Clinical Manifestations and Neuroradiological Features. Clin Neuroradiol 2019;29:3-18.
7. Baloji A, Ghasi RG. MRI in intracranial tuberculosis: Have we seen it all? Clin Imaging 2020;68:263-77.
8. Rogerio F, de Souza Queiroz L, Reis F, Fukuda A, Silva NA Jr, Joaquim AF. A 32-Year-Old Man with Headache and Visual Loss. Brain Pathol 2017;27:559-60.
9. Amin S, Stone D, Anderlind C. A 32-Year-Old Woman With Miscarriage, Headache, Hepatitis, and Pulmonary Disease. Chest 2019;155:e101-5.
10. Churchyard G, Kim P, Shah NS, Rustomjee R, Gandhi N, Mathema B, Dowdy D, Kasmar A, Cardenas V. What We Know About Tuberculosis Transmission: An Overview. J Infect Dis 2017;216:S629-35.
11. Maramattom BV, Santhamma SGN. Tuberculous Encephalitis May Be Undetectable on Magnetic Resonance Imaging but Detectable on 18F-Fluorodeoxyglucose Positron Emission Tomography-Computed Tomography. Am J Trop Med Hyg 2021;105:1031-7.
12. Kong C, Xu D, Wang Y, Wang B, Wen J, Wang X, Zhan L, Sun Z, Jia X, Li M, Tang S, Hou D. Amplitude of low-frequency fluctuations in multiple-frequency bands in patients with intracranial tuberculosis: a prospective cross-sectional study. Quant Imaging Med Surg 2022;12:4120-34.
13. Feng M, Wen H, Xin H, Zhang N, Liang C, Guo L. Altered Spontaneous Brain Activity Related to Neurologic Dysfunction in Patients With Cerebral Small Vessel Disease. Front Aging Neurosci 2021;13:731585.
14. Prodoehl J, Burciu RG, Vaillancourt DE. Resting state functional magnetic resonance imaging in Parkinson's disease. Curr Neurol Neurosci Rep 2014;14:448.
15. Su T, Yuan Q, Liao XL, Shi WQ, Zhou XZ, Lin Q, Min YL, Li B, Jiang N, Shao Y. Altered intrinsic functional connectivity of the primary visual cortex in patients with retinal vein occlusion: a resting-state fMRI study. Quant Imaging Med Surg 2020;10:958-69.
16. Chen SY, Cai GQ, Liang RB, Yang QC, Min YL, Ge QM, Li B, Shi WQ, Li QY, Zeng XJ, Shao Y. Regional brain changes in patients with diabetic optic neuropathy: a resting-state functional magnetic resonance imaging study. Quant Imaging Med Surg 2021;11:2125-37.
17. Zang Y, Jiang T, Lu Y, He Y, Tian L. Regional homogeneity approach to fMRI data analysis. Neuroimage 2004;22:394-400.
18. Zuo XN, Xu T, Jiang L, Yang Z, Cao XY, He Y, Zang YF, Castellanos FX, Milham MP. Toward reliable characterization of functional homogeneity in the human brain: preprocessing, scan duration, imaging resolution and computational space. Neuroimage 2013;65:374-86.
19. He Y, Wang L, Zang Y, Tian L, Zhang X, Li K, Jiang T. Regional coherence changes in the early stages of Alzheimer's disease: a combined structural and resting-state functional MRI study. Neuroimage 2007;35:488-500.
20. Li HJ, Cao XH, Zhu XT, Zhang AX, Hou XH, Xu Y, Zuo XN, Zhang KR. Surface-based regional homogeneity in first-episode, drug-naïve major depression: a resting-state FMRI study. Biomed Res Int 2014;2014:374828.
21. Lv H, Wang Z, Tong E, Williams LM, Zaharchuk G, Zeineh M, Goldstein-Piekarski AN, Ball TM, Liao C, Wintermark M. Resting-State Functional MRI: Everything That Nonexperts Have Always Wanted to Know. AJNR Am J Neuroradiol 2018;39:1390-9.
22. Wu QZ, Li DM, Kuang WH, Zhang TJ, Lui S, Huang XQ, Chan RC, Kemp GJ, Gong QY. Abnormal regional spontaneous neural activity in treatment-refractory depression revealed by resting-state fMRI. Hum Brain Mapp 2011;32:1290-9.
23. Vachha BA, Gohel S, Root JC, Kryza-Lacombe M, Hensley ML, Correa DD. Altered regional homogeneity

in patients with ovarian cancer treated with chemotherapy: a resting state fMRI study. Brain Imaging Behav 2022;16:539-46.
24. Zhang G, Cheng Y, Shen W, Liu B, Huang L, Xie S. Brain Regional Homogeneity Changes in Cirrhotic Patients with or without Hepatic Encephalopathy Revealed by Multi-Frequency Bands Analysis Based on Resting-State Functional MRI. Korean J Radiol 2018;19:452-62.
25. Pan P, Zhan H, Xia M, Zhang Y, Guan D, Xu Y. Aberrant regional homogeneity in Parkinson's disease: A voxel-wise meta-analysis of resting-state functional magnetic resonance imaging studies. Neurosci Biobehav Rev 2017;72:223-31.
26. Jiang L, Zuo XN. Regional Homogeneity: A Multimodal, Multiscale Neuroimaging Marker of the Human Connectome. Neuroscientist 2016;22:486-505.
27. Zuo XN, Xing XX. Test-retest reliabilities of resting-state FMRI measurements in human brain functional connectomics: a systems neuroscience perspective. Neurosci Biobehav Rev 2014;45:100-18.
28. Li Z, Kadivar A, Pluta J, Dunlop J, Wang Z. Test-retest stability analysis of resting brain activity revealed by blood oxygen level-dependent functional MRI. J Magn Reson Imaging 2012;36:344-54.
29. Berboth S, Windischberger C, Kohn N, Morawetz C. Test-retest reliability of emotion regulation networks using fMRI at ultra-high magnetic field. Neuroimage 2021;232:117917.
30. Zhang Z, Liu Y, Jiang T, Zhou B, An N, Dai H, Wang P, Niu Y, Wang L, Zhang X. Altered spontaneous activity in Alzheimer's disease and mild cognitive impairment revealed by Regional Homogeneity. Neuroimage 2012;59:1429-40.
31. Guo WB, Liu F, Xue ZM, Yu Y, Ma CQ, Tan CL, Sun XL, Chen JD, Liu ZN, Xiao CQ, Chen HF, Zhao JP. Abnormal neural activities in first-episode, treatment-naïve, short-illness-duration, and treatment-response patients with major depressive disorder: a resting-state fMRI study. J Affect Disord 2011;135:326-31.
32. Liu CH, Ma X, Wu X, Zhang Y, Zhou FC, Li F, Tie CL, Dong J, Wang YJ, Yang Z, Wang CY. Regional homogeneity of resting-state brain abnormalities in bipolar and unipolar depression. Prog Neuropsychopharmacol Biol Psychiatry 2013;41:52-9.
33. Liu P, Li Q, Zhang A, Liu Z, Sun N, Yang C, Wang Y, Zhang K. Similar and Different Regional Homogeneity Changes Between Bipolar Disorder and Unipolar Depression: A Resting-State fMRI Study. Neuropsychiatr Dis Treat 2020;16:1087-93.
34. Yin D, Luo Y, Song F, Xu D, Peterson BS, Sun L, Men W, Yan X, Fan M. Functional reorganization associated with outcome in hand function after stroke revealed by regional homogeneity. Neuroradiology 2013;55:761-70.
35. Zhao Z, Tang C, Yin D, Wu J, Gong J, Sun L, Jia J, Xu D, Fan M. Frequency-specific alterations of regional homogeneity in subcortical stroke patients with different outcomes in hand function. Hum Brain Mapp 2018;39:4373-84.
36. Matsuda H. Role of neuroimaging in Alzheimer's disease, with emphasis on brain perfusion SPECT. J Nucl Med 2007;48:1289-300.
37. Chételat G, Eustache F, Viader F, De La Sayette V, Pélerin A, Mézenge F, Hannequin D, Dupuy B, Baron JC, Desgranges B. FDG-PET measurement is more accurate than neuropsychological assessments to predict global cognitive deterioration in patients with mild cognitive impairment. Neurocase 2005;11:14-25.
38. Liu Y, Wang K, Yu C, He Y, Zhou Y, Liang M, Wang L, Jiang T. Regional homogeneity, functional connectivity and imaging markers of Alzheimer's disease: a review of resting-state fMRI studies. Neuropsychologia 2008;46:1648-56.
39. Fox MD, Raichle ME. Spontaneous fluctuations in brain activity observed with functional magnetic resonance imaging. Nat Rev Neurosci 2007;8:700-11.
40. Buzsáki G, Draguhn A. Neuronal oscillations in cortical networks. Science 2004;304:1926-9.
41. Zuo XN, Di Martino A, Kelly C, Shehzad ZE, Gee DG, Klein DF, Castellanos FX, Biswal BB, Milham MP. The oscillating brain: complex and reliable. Neuroimage 2010;49:1432-45.
42. Salvador R, Martínez A, Pomarol-Clotet E, Gomar J, Vila F, Sarró S, Capdevila A, Bullmore E. A simple view of the brain through a frequency-specific functional connectivity measure. Neuroimage 2008;39:279-89.
43. Zhang S, Li H, Xu Q, Wang C, Li X, Sun J, Wang Y, Sun T, Wang Q, Zhang C, Wang J, Jia X, Sun X. Regional homogeneity alterations in multi-frequency bands in tension-type headache: a resting-state fMRI study. J Headache Pain 2021;22:129.
44. China National Health and Family Planning Commission of the People's Republic of China (2018b). Diagnosis for pulmonary tuberculosis (WS 288-2017). Chin J Infect Control 2018;17:642-52
45. World Health Organization. Global tuberculosis report 2017. Available online: http://www.who.int/tb/

publications/global_report/en/
46. Rodriguez-Takeuchi SY, Renjifo ME, Medina FJ. Extrapulmonary Tuberculosis: Pathophysiology and Imaging Findings. Radiographics 2019;39:2023-37.
47. Folstein MF, Folstein SE, McHugh PR. "Mini-mental state". A practical method for grading the cognitive state of patients for the clinician. J Psychiatr Res 1975;12:189-98.
48. Nasreddine ZS, Phillips NA, Bédirian V, Charbonneau S, Whitehead V, Collin I, Cummings JL, Chertkow H. The Montreal Cognitive Assessment, MoCA: a brief screening tool for mild cognitive impairment. J Am Geriatr Soc 2005;53:695-9.
49. Bowie CR, Harvey PD. Administration and interpretation of the Trail Making Test. Nat Protoc 2006;1:2277-81.
50. Shulman KI. Clock-drawing: is it the ideal cognitive screening test? Int J Geriatr Psychiatry 2000;15:548-61.
51. Shao Z, Janse E, Visser K, Meyer AS. What do verbal fluency tasks measure? Predictors of verbal fluency performance in older adults. Front Psychol 2014;5:772.
52. Lezak MD, Howison DB, Loring DW. Neuropsychological assessment. 4th edition. New York: Oxford University Press, 2004.
53. Jia XZ, Wang J, Sun HY, Zhang H, Liao W, Wang Z, Yan CG, Song XW, Zang YF. RESTplus: an improved toolkit for resting-state functional magnetic resonance imaging data processing. Science Bulletin 2019;64:953-4.
54. Friston KJ, Williams S, Howard R, Frackowiak RS, Turner R. Movement-related effects in fMRI time-series. Magn Reson Med 1996;35:346-55.
55. Bardeen JM, Bond JR, Kaiser N, Szalay AS. The statistics of peaks of Gaussian random fields. Astrophys J 1986;304. doi: 10.1086/164143.
56. Snyder P, Lawson S. Evaluating Results Using Corrected and Uncorrected Effect Size Estimates. J Exp Educ 1993;61:334-49.
57. Tzourio-Mazoyer N, Landeau B, Papathanassiou D, Crivello F, Etard O, Delcroix N, Mazoyer B, Joliot M. Automated anatomical labeling of activations in SPM using a macroscopic anatomical parcellation of the MNI MRI single-subject brain. Neuroimage 2002;15:273-89.
58. Fu J, Chen X, Gu Y, Xie M, Zheng Q, Wang J, Zeng C, Li Y. Functional connectivity impairment of postcentral gyrus in relapsing-remitting multiple sclerosis with somatosensory disorder. Eur J Radiol 2019;118:200-6.
59. Kropf E, Syan SK, Minuzzi L, Frey BN. From anatomy to function: the role of the somatosensory cortex in emotional regulation. Braz J Psychiatry 2019;41:261-9.
60. Ismail Y. Pulmonary tuberculosis--a review of clinical features and diagnosis in 232 cases. Med J Malaysia 2004;59:56-64.
61. Tang LY, Li HJ, Huang X, Bao J, Sethi Z, Ye L, Yuan Q, Zhu PW, Jiang N, Gao GP, Shao Y. Assessment of synchronous neural activities revealed by regional homogeneity in individuals with acute eye pain: a resting-state functional magnetic resonance imaging study. J Pain Res 2018;11:843-50.
62. Frot M, Magnin M, Mauguière F, Garcia-Larrea L. Cortical representation of pain in primary sensory-motor areas (S1/M1)--a study using intracortical recordings in humans. Hum Brain Mapp 2013;34:2655-68.
63. Dou Z, Zhang X, Yang L, Wang W, Li N, Liu Z, Ni J. Alternation of regional homogeneity in trigeminal neuralgia after percutaneous radiofrequency thermocoagulation: A resting state fMRI study. Medicine (Baltimore) 2016;95:e5193.
64. Ma M, Zhang H, Liu R, Liu H, Yang X, Yin X, Chen S, Wu X. Static and Dynamic Changes of Amplitude of Low-Frequency Fluctuations in Cervical Discogenic Pain. Front Neurosci 2020;14:733.
65. Yang J, Li B, Yu QY, Ye L, Zhu PW, Shi WQ, Yuan Q, Min YL, He YL, Shao Y. Altered intrinsic brain activity in patients with toothaches using the amplitude of low-frequency fluctuations: a resting-state fMRI study. Neuropsychiatr Dis Treat 2019;15:283-91.
66. Xie YJ, Xi YB, Cui LB, Guan MZ, Li C, Wang ZH, Fang P, Yin H. Functional connectivity of cerebellar dentate nucleus and cognitive impairments in patients with drug-naive and first-episode schizophrenia. Psychiatry Res 2021;300:113937.
67. Bogler C, Vowinkel A, Zhutovsky P, Haynes JD. Default Network Activity Is Associated with Better Performance in a Vigilance Task. Front Hum Neurosci 2017;11:623.
68. Chen HL, Lu CH, Chang CD, Chen PC, Chen MH, Hsu NW, Chou KH, Lin WM, Lin CP, Lin WC. Structural deficits and cognitive impairment in tuberculous meningitis. BMC Infect Dis 2015;15:279.
69. Lara-Espinosa JV, Santana-Martínez RA, Maldonado PD, Zetter M, Becerril-Villanueva E, Pérez-Sánchez G, Pavón L, Mata-Espinosa D, Barrios-Payán J, López-Torres MO, Marquina-Castillo B, Hernández-Pando R. Experimental Pulmonary Tuberculosis in the Absence of Detectable Brain Infection Induces Neuroinflammation and Behavioural Abnormalities in Male BALB/c Mice. Int J Mol Sci 2020.
70. Wandell BA, Dumoulin SO, Brewer AA. Visual field maps

in human cortex. Neuron 2007;56:366-83.
71. Xiang CQ, Liu WF, Xu QH, Su T, Yong-Qiang S, Min YL, Yuan Q, Zhu PW, Liu KC, Jiang N, Ye L, Shao Y. Altered Spontaneous Brain Activity in Patients with Classical Trigeminal Neuralgia Using Regional Homogeneity: A Resting-State Functional MRI Study. Pain Pract 2019;19:397-406.
72. Zhang YQ, Zhu FY, Tang LY, Li B, Zhu PW, Shi WQ, Lin Q, Min YL, Shao Y, Zhou Q. Altered regional homogeneity in patients with diabetic vitreous hemorrhage. World J Diabetes 2020;11:501-13.
73. Abdisamadov A, Tursunov O. Ocular tuberculosis epidemiology, clinic features and diagnosis: A brief review. Tuberculosis (Edinb) 2020;124:101963.
74. Leonard JM. Central Nervous System Tuberculosis. Microbiol Spectr 2017.
75. Lee C, Agrawal R, Pavesio C. Ocular Tuberculosis--A Clinical Conundrum. Ocul Immunol Inflamm 2016;24:237-42.
76. Cui Y, Jiao Y, Chen YC, Wang K, Gao B, Wen S, Ju S, Teng GJ. Altered spontaneous brain activity in type 2 diabetes: a resting-state functional MRI study. Diabetes 2014;63:749-60.
77. Baillieux H, De Smet HJ, Dobbeleir A, Paquier PF, De Deyn PP, Mariën P. Cognitive and affective disturbances following focal cerebellar damage in adults: a neuropsychological and SPECT study. Cortex 2010;46:869-79.
78. de Oliveira Wertheimer GS, Rossi Assis-Mendonça G, de Souza Queiroz L, Reis F. Mycobacterium infection as a mimicker of brain metastasis. Clin Case Rep 2021;9:2481-2.
79. Di Martino A, Ross K, Uddin LQ, Sklar AB, Castellanos FX, Milham MP. Functional brain correlates of social and nonsocial processes in autism spectrum disorders: an activation likelihood estimation meta-analysis. Biol Psychiatry 2009;65:63-74.
80. Han Y, Wang J, Zhao Z, Min B, Lu J, Li K, He Y, Jia J. Frequency-dependent changes in the amplitude of low-frequency fluctuations in amnestic mild cognitive impairment: a resting-state fMRI study. Neuroimage 2011;55:287-95.
81. Méchaï F, Bouchaud O. Tuberculous meningitis: Challenges in diagnosis and management. Rev Neurol (Paris) 2019;175:451-7.
82. Ma J, Hua XY, Zheng MX, Wu JJ, Huo BB, Xing XX, Feng SY, Li B, Xu JG. Surface-based map plasticity of brain regions related to sensory motor and pain information processing after osteonecrosis of the femoral head. Neural Regen Res 2022;17:806-11.
83. Zhang B, Wang F, Dong HM, Jiang XW, Wei SN, Chang M, Yin ZY, Yang N, Zuo XN, Tang YQ, Xu K. Surface-based regional homogeneity in bipolar disorder: A resting-state fMRI study. Psychiatry Res 2019;278:199-204.

Cite this article as: Wang Y, Wen J, Kong C, Xu Z, Hu S, Li M, Wang X, Zhang H, Jia X, Ding Q, Wu J, Hou D. Regional homogeneity alterations in multifrequency bands in patients with extracranial multi-organ tuberculosis: a prospective cross-sectional study. Quant Imaging Med Surg 2023;13(3):1753-1767. doi: 10.21037/qims-22-229

